HHS Public Access

Author manuscript

Clin Sci (Lond). Author manuscript; available in PMC 2023 January 19.

Published in final edited form as:

Clin Sci (Lond). 2022 May 27; 136(10): 715–731. doi:10.1042/CS20220188.

Angiotensin II Type-2-Receptor Stimulation Ameliorates Focal and Segmental Glomerulosclerosis in Mice

Min-Chun Liao[1,*], **Kana N. Miyata**[1,2,*], **Shiao-Ying Chang**[1], **Xin-Ping Zhao**[1], **Chao-Sheng Lo**[1], **Mohamad-Ali El-Mortada**[1], **Junzheng Peng**[1], **Isabelle Chenier**[1], **Michifumi Yamashita**[3], **Julie R. Ingelfinger**[4], **John S. D. Chan**[1], **Shao-Ling Zhang**[1,§]

[1]Department of Medicine, Université de Montréal, Centre de recherche du Centre hospitalier de l'Université de Montréal (CRCHUM), 900 Saint Denis Street, Montréal, QC, Canada H2X 0A9

[2]Division of Nephrology, Department of Internal Medicine, Saint Louis University, 1008 Spring Ave. St Louis, MO, U.S.A. 63110

[3]Department of Pathology and Laboratory Medicine, Cedars-Sinai Medical Center, 8700 Beverly Blvd, Los Angeles, CA, U.S.A. 90048

[4]Pediatric Nephrology Unit, Mass General Hospital *for* Children at Massachusetts General Hospital, Harvard Medical School, 55 Fruit Street, Boston, MA, U.S.A. 02114

Abstract

Podocyte damage and loss are the early event in the development of focal segmental glomerulosclerosis (FSGS). Podocytes express angiotensin II type-2-receptor (AT_2R), which may play a key role in maintaining kidney integrity and function. Here, we examined the effects of AT_2R deletion and AT_2R agonist compound 21 (C21) on the evolution of FSGS. FSGS was induced by adriamycin (ADR) injection in both male wild-type (WT) and AT_2R knock-out (KO) mice. C21 was administered to WT-FSGS mice either one day before or 7 days after ADR (Pre-C21 or Post-C21), using two doses of C21 at either 0.3 (low dose, LD) or 1.0 (high dose, HD) mg/kg/day. ADR-induced FSGS was more severe in AT_2RKO mice compared with WT-FSGS mice, and included profound podocyte loss, glomerular fibrosis, and albuminuria. Glomerular cathepsin L expression increased more in AT_2RKO-FSGS than in WT-FSGS mice.

[§]To whom correspondence should be addressed: Shao-Ling Zhang, Ph.D., Tel: (514) 890-8000 ext. 15633, Fax: (514) 412-7655, shao.ling.zhang@umontreal.ca.

[*]Liao MC and Miyata KN contributed equally

Disclosure

The authors declare no conflict of interests.

CRediT Author Contribution

Min-Chun Liao: Conceptualization, Data curation, Formal analysis, Methodology, Investigation, Project administration, Visualization, Writing – review & editing. **Kana N. Miyata**: Conceptualization, Formal analysis, Methodology, Project administration, Visualization, Writing – original draft. **Shiao-Ying Chang**: Data curation, Formal analysis, Investigation, Writing – review & editing. **Xin-Ping Zhao**: Data curation, Formal analysis, Investigation, Writing – review & editing. **Chao-Sheng Lo**: Data curation, Formal analysis, Investigation, Writing – review & editing. **Mohamad-Ali El-Mortada**: Data curation, Investigation, Formal analysis, Writing – review & editing. **Junzheng Peng**: Investigation, Resources, Writing – review & editing. **Isabelle Chenier**: Data curation, Investigation, Project administration, Formal analysis, Writing – review & editing. **Michifumi Yamashita**: Investigation, Resources, Writing – review & editing. **Julie R. Ingelfinger**: Conceptualization, Formal analysis, Methodology, Supervision, Writing – review & editing. **John S. D. Chan**: Conceptualization, Formal analysis, Funding acquisition, Methodology, Resources, Supervision, Writing – review & editing. **Shao-Ling Zhang**: Conceptualization, Formal analysis, Funding acquisition, Methodology, Resources, Supervision, Writing – review & editing.

C21 treatment ameliorated podocyte injury, most significantly in the Pre C21-HD group, and inhibited glomerular cathepsin L expression. *In vitro*, Agtr2 knock-down in mouse podocyte cell line given ADR confirmed the *in vivo* data. Mechanistically, C21 inhibited cathepsin L expression, which protected synaptopodin from destruction and stabilized actin cytoskeleton. C21 also prevented podocyte apoptosis. In conclusion, AT_2R activation by C21 ameliorated ADR-induced podocyte injury in mice by the inhibition of glomerular cathepsin L leading to the maintenance of podocyte integrity and prevention of podocyte apoptosis.

Keywords

AT_2R; C21; cathepsin L; FSGS; podocyte

INTRODUCTION

Classical focal segmental glomerulosclerosis (FSGS) is initiated by podocyte injury. Microscopy reveals areas of glomerular sclerosis associated with interstitial fibrosis and tubular atrophy [1]. The prevalence of FSGS is increasing worldwide and it constitutes a major glomerular cause of end stage kidney disease [2–4]. Thus, the innovative targeted therapies that will require a better understanding of the molecular mechanisms of podocyte injury and how podocyte injury leads to glomerulosclerosis and proteinuria are of high interest.

The renin-angiotensin-system (RAS) plays an important role as a mediator of kidney injury in FSGS [5, 6]. Angiotensin II (Ang II) acts through two major subtypes of angiotensin receptors, angiotensin II type-1-receptor (AT_1R) and angiotensin II type-2-receptor (AT_2R). In general, AT_1R activation induces vasoconstriction, cellular dedifferentiation, proliferation, fibrosis, and anti-natriuresis, while AT_2R activation induces vasodilation, cellular differentiation, anti-proliferation, anti-fibrosis, and natriuresis [7, 8]. Studies have shown that podocytes generate RAS components locally, including AT_1R and AT_2R [9–12]. AT_1R blockers are a mainstay of FSGS therapy, leading to decrease in proteinuria, independent of hemodynamic actions [13–15]. Beyond the alteration of intraglomerular pressure, Ang II directly causes podocyte apoptosis via AT_1R [16, 17] and stimulates type IV collagen production in podocytes through increased TGF-β and vascular endothelial growth factor signaling [18]. Despite accumulating evidence supporting the use of AT_1R blockers in FSGS, little is known about the effects of AT_2R activators, which have been reported to protect the kidney in multiple other disease models, either by direct action or by virtue of counteracting AT_1R-mediated deleterious effects [19–21].

Podocytes express AT_2R and play a key role in maintaining the integrity and function of the glomerular filtration barrier [9, 10, 12]. We previously reported that AT_2R is essential in normal glomerulogenesis *in vivo* and *in vitro* [9, 10]. Embryonic kidneys lacking AT_2R display features of renal dysplasia with lower glomerular tuft volume and podocyte numbers, and both AT_2R siRNA and the AT_2R antagonist (PD123319) decreased synaptopodin (Synpo) expression in an immortalized mouse podocyte cell line (mPODs). While AT_2R is only sparsely expressed in healthy adult kidneys, it is reportedly up-regulated in pathological

conditions, such as obesity, diabetes, Ang II-induced hypertension, folic acid nephropathy, and protein overload proteinuria [22–24]. Moreover, the effects of the selective, nonpeptide AT_2R agonist, compound 21 (C21), suggest that AT_2R might be a potential target for protection against hypertension, metabolic dysfunction and organ remodeling [21]. Though C21 has been reported to improve kidney function (evaluated by proteinuria scoring and estimated glomerular filtration rate) in kidney of high-salt–fed obese Zucker rats [25], little is known about the efficacy and the renoprotective action of C21 in glomerular diseases or specifically in podocytes.

Here, we hypothesized that AT_2R may exert a protective action on podocyte injury in FSGS. To test our hypothesis, we used adriamycin (ADR) nephropathy, a well-characterized murine model of human FSGS, which is marked by prominent podocyte injury, glomerular fibrosis, and proteinuria [26]. Our present study aimed to investigate the effect of AT_2R knock-out (KO) on the development of ADR-induced FSGS, as well as the efficacy and the mechanism by which C21 ameliorated experimental murine FSGS. We found that C21 did so through the inhibition of glomerular cathepsin L (a lysosomal cysteine proteinase expressed in podocytes [27, 28]), leading to the maintenance of podocyte integrity.

METHODS

Animal Models

AT_2RKO mice (C57BL/6) [29, 30] were kindly provided by Dr. Tadashi Inagami (Vanderbilt University School of Medicine, Nashville, TN, USA); we have reported their use elsewhere [10, 31]. Wild-type (WT, C57BL/6) mice served as controls (WT-Con). FSGS was induced in both male WT-Con and AT_2RKO-Con mice at 8 weeks of age by intravenous (i.v.) injection of ADR (doxorubicin, 18 mg/kg, body weight (BW), in saline; Cayman Chemical Company, Ann Arbor, Michigan, USA). C21 (a gift from Vicore Pharma, Göteborg Sweden) was administered to WT-FSGS mice either one day before or 7 days after ADR injection; C21 was given as either 0.3 (low dose, LD) or 1.0 (high dose, HD) mg/kg (BW)/day via intraperitoneal (i.p.) injection, in saline. Note, the subgroups were called Pre C21-LD or Pre C21-HD; and Post C21-LD or Post C21-HD. We used male mice as male rodents are more susceptible than females to ADR-induced nephropathy [32, 33]. Mice were euthanized 4 weeks after ADR injection by injection of 75 mg/kg sodium pentobarbital (i.p.), and the kidneys were removed immediately. The detailed experimental protocol is shown in Figure 1A.

Animal care and experimental procedures were approved by the Animal Care Committee at the Centre de recherche du centre hospitalier de l’ Université de Montréal (Protocol# CM18049SZs, CRCHUM). The animals were housed in ventilated cages in SPF conditions under a 12-hour, light-dark cycle with free access to chow and water at the CRCHUM’s animal facility.

Mouse Physiological Studies

Body weight (BW, g) was recorded weekly. Kidney weight (KW, g) and tibia length (TL, mm) were recorded when the animals were euthanized. Systolic blood pressure was

monitored by tail-cuff at 12 weeks of age following one week of pre-training using a BP-2000 Blood Pressure Analysis System (Visitech Systems Inc., Apex, NC), as reported elsewhere [34, 35].

Urinary Measurements

Urine samples were collected from mice individually housed in metabolic cages. Urinary albumin/creatinine ratio (mg/mmol) (Albuwell and Creatinine Companion, Exocell Inc., Philadelphia, PA, USA) was determined biweekly post-ADR injection by ELISA and normalized by urinary creatinine levels as described [10, 34]. Urinary albumin level was also estimated by Coomassie Blue gel staining of electrophoresed urine samples as reported. [10, 34] Urinary Ang II /creatinine ratio (pmol/μmol) (Immuno-Biological Laboratories, IBL America, Minneapolis, MN, USA) was assayed by ELISA and normalized by urinary creatinine levels as described.[34, 35]

Kidney Morphology and Podocyte Number

Kidneys were either quickly frozen in OCT or fixed overnight in 4% paraformaldehyde at 4°C before paraffin-embedding. Kidney morphology was assessed in sections stained with periodic acid Schiff (PAS) and Masson trichrome [10, 34]. Glomerulosclerosis (based on PAS images, semi-quantitative scale from 0 to 4) was scored by a person blinded to the experimental group. Both immunohistochemistry (IHC) and immunofluorescence (IF) were performed using standard protocols [10, 34]. The sources of antibodies used are listed in Supplementary Table S1. Relative staining intensity and area were quantified using the 2-D staining images (N=4–6 mice/group) in a blinded fashion. Brightness and contrast were adjusted on displayed images (identically for compared image sets) and quantified (identical threshold settings for compared image sets) using NIH Image J software (Bethesda, MD, USA). Podocyte number per glomerular area (number per μm^2) was analyzed in a blinded fashion by counting p57 positively nuclear stained cells in glomerular-cross sections (30–35 glomeruli/mouse, N=4–6 mice/group) [10, 34].

Electron Microscopy

Kidney tissues fixed in 3% glutaraldehyde were postfixed in OsO_4 and embedded in epoxy resin. Ultrathin sections were stained with uranyl acetate and lead citrate, as previously described [36]. Micrographs were taken using Hitachi 7700 transmission electron microscope (Hitachi, Santa Clara, CA).

Real Time-Quantitative Polymerase Chain Reaction (RT-qPCR)

7500 Fast real-time PCR system (Applied Biosystems, Mississauga, Canada) was performed in glomeruli isolated by using iron oxide beads (2.5mg/ml) with the aid of a magnet concentrator [10, 34]. The mRNA change in each gene was determined and normalized to its own *Rpl13a* mRNA, and the percentage change was compared with the expression of the corresponding gene in male WT-Con (1 in fold change) vs. the rest of the subgroups by using the $2^{(-\Delta\Delta CT)}$ method. The primers used are shown in Supplementary Table S2.

Podocyte Culture

An immortalized mouse podocyte cell line (mPOD) was kindly donated by Dr. Stuart J. Shankland (University of Washington, WA, USA) [37]; we previously reported their use in our studies [9, 10]. Agtr2 siRNA (vs. scrambled siRNA) (50 nmol/l) was used to knock-down Agtr2 expression in mPODs. Cells were treated with different doses of C21 (0, 0.1 μM, and 1.0 μM) for 24 hours.

Statistical Analysis

For the animal studies, groups of 8 to 20 mice were used (N.B., the precise number of animals used for each specific experiment is either labeled on the figures or shown as individual data points on column scatter graphs). Statistical significance between the experimental groups was analyzed using Prism 6.0 software (GraphPad, San Diego, CA), by 1-way ANOVA followed by the Bonferroni's *post hoc* test (*in vivo* studies). A probability level of $p < 0.05$ was considered statistically significant [9, 10].

RESULTS

AT_2R Deletion Exacerbated and C21 Ameliorated Adriamycin-induced FSGS

Figure 1A details the FSGS experimental protocols performed in both WT and AT_2RKO mice, as well as the treatment of AT_2R agonist, C21 (LD vs. HD; Pre-C21 vs. Post-C21) on WT-FSGS mice. Deletion of AT_2R (AT_2RKO-Con) did not change BW compared with WT-Con mice. Adriamycin injection led to similar degrees of weight loss in both WT-FSGS and AT_2RKO-FSGS mice (Figure 1B); C21 treatment did not prevent the ADR-induced weight loss (Figure 1C). AT_2RKO mice had increased systolic blood pressure (SBP) compared to WT-Con mice, and SBP was further increased in both WT-FSGS and AT_2RKO-FSGS (Figure 1D). In contrast, ADR-induced hypertension was significantly decreased in all C21 treatment groups (Pre C21-LD/HD and Post C21-LD/HD), in a dose-dependent manner, particularly in Pre-C21 groups (Figure 1E). The KW/TL ratio remained similar between WT-Con and AT_2RKO-Con, and it was decreased in both WT-FSGS and AT_2RKO-FSGS (Figure 1F); the decreased ratio was unchanged by C21 treatment (Figure 1G).

Urinary albumin/creatinine ratio (ACR) was significantly increased in WT-FSGS compared to WT-Con, and was further increased in AT_2RKO-FSGS both 2 weeks and 4 weeks after ADR injection (Figure 2A and Supplementary Figure S1). Pre-C21 treatment greatly improved urinary ACR in both LD and HD groups (Figure 2B and Supplementary Figure S1). Coomassie Blue gel staining further confirmed those urinary albumin levels at both 2 weeks (Figure 2C–2D) and 4 weeks (Figure 2E–2F) after ADR injection. Urinary Ang II was increased in FSGS mice with and without AT_2RKO (Figure 2G), and it was unaltered by C21 treatments (Figure 2H).

PAS (Figure 3A–3D) and Masson trichrome (Figure 3E–3H) staining of the renal cortex showed no remarkable pathological changes in AT_2RKO-Con mice compared to WT-Con. However, WT-FSGS mice developed obvious glomerular segmental sclerosis, and this was far more severe in AT_2RKO-FSGS (Figure 3A–3B; 3E–3F). In contrast, C21 treatment (LD vs. HD; Pre-C21 vs. Post-C21) significantly improved those morphological features (Figure

3D; 3H). Regardless of dose, Pre-C21 was more effective than Post-C21; and Post-C21 groups showed a dose-dependent manner (Figure 3D; 3H).

Glomerular Molecular Changes in AT_2RKO-FSGS and WT-FSGS with C21 Treatment

We investigated whether glomerular gene expression related to apoptotic and profibrotic processes was altered in these mice. Both WT-Con and AT_2RKO-Con mice had similar basal mRNA expression of certain genes (Figure 4A, *Bax* and *Bcl2*; Figure 4C, *Tgf-β1* and *Col4α1*) in isolated glomeruli. Compared to the respective controls, mRNA expression of *Bax*, *Tgf-β1* and *Col4α1* was up-regulated, and *Bcl2* mRNA expression was down-regulated in the glomeruli of ADR mice. There were no significant differences in the expression of these mRNAs between WT-FSGS and AT_2RKO-FSGS mice (Figure 4A; 4C). In contrast, C21 treatment (LD vs. HD; Pre-C21 vs. Post-C21) attenuated the changes of both *Bax* and *Bcl2* (Figure 4B); and reduced *Tgf-β1* and *Col4α1* mRNA expression in WT-FSGS mice (Figure 4D).

TUNEL assay (Figure 4E) confirmed apoptotic changes; WT-FSGS and AT_2RKO-FSGS mice exhibited a profound increase in the number of cells stained with TUNEL in glomeruli as compared to control animals. C21 significantly reduced the number of TUNEL-stained cells in all the treatment groups (Figure 4F). Similarly, collagen IV-IHC reversed the glomerular profibrotic pattern in ADR mice; collagen IV expression was increased in WT-FSGS mice, which was further increased in AT_2RKO-FSGS mice (Figure 4G). C21 treatment ameliorated the collagen IV expressions (Figure 4H).

Podocyte Molecular Changes in AT_2RKO-FSGS and WT-FSGS with C21 Treatment

Normal podocyte foot processes were observed in WT-Con and AT_2RKO-Con mice through electron microscopic study (Figure 5A). WT-FSGS and AT_2RKO-FSGS mice had extensive foot process effacement, which were ameliorated by C21 treatment (Figure 5B).

The mRNA expressions of podocyte-specific markers, Wilms tumor 1 (Wt-1) and Synpo, were similarly downregulated in isolated glomeruli of WT-FSGS and AT_2RKO-FSGS mice (Figure 5C). These changes were reduced by C21 treatment, most significantly in Pre C21-HD group (Figure 5D). In WT-Con mice, there was a linear staining of Synpo along the glomerular capillary loop, which was reduced in AT_2RKO-Con (Figure 5E). Synpo staining was further reduced in WT-FSGS (Figure 5E). Synpo staining was even more reduced in AT_2RKO-FSGS and became uneven throughout the glomerulus (Figure 5E). C21 treatment appeared to reverse the changes seen on Synpo staining, dose dependently (Figure 5F).

The number of podocytes, counted as p57 positive nuclei in glomeruli, were significantly reduced by approximately 40% both in WT-FSGS and AT_2RKO-FSGS (Figure 5G), and were increased by C21 treatment, most significantly in Pre C21-HD group (Figure 5H).

AT_2R plays a key role in reducing the production of proinflammatory cytokines [38]. We measured the mRNA expressions for a panel of cytokines in isolated glomeruli. ADR stimulated the glomerular expressions of C–C motif chemokine ligand 2 (*Ccl2*), tumor necrosis factor-α (*TNF-α*), *interleukin (IL)-1β*, and *IL-6* (Figure 6A), which is consistent with previous literatures [39]. Moreover, *Ccl2* expression in AT_2RKO-FSGS mice were

further increased compared to the one in WT-FSGS mice. Interestingly, there was a significant reduction of Ccl2, *TNF-α*, and *IL-1β* expressions by C21 treatment (Figure 6B). There was no difference in *IL-10* expression either in WT-FSGS or AT_2RKO-FSGS mice compared to WT-Cont, but it was increased by C21 treatment, most significantly in Pre-C21-HD group (Figure 6B).

Cathepsin L Expression is Increased by ADR and Reduced by C21 Treatment

It has been suggested that inflammatory cytokines are related to cathepsin L induction [40]. Therefore, we hypothesized that Cathepsin L expression may be altered via AT_2R. Cathepsin L-IF expression was observed mainly in glomerular parietal epithelial cells of WT-Con and AT_2RKO mice, but the Cathepsin L was also positively stained in the cells along the capillary loop in the glomeruli from WT-FSGS mice, most prominently in AT_2RKO-FSGS mice (Figure 6C). Co-staining of cathepsin L and Synpo indicated that cathepsin L emerged in podocytes after ADR injection (Figure 6C; 6E). Intriguingly, C21 treatment reduced the podocyte expression of cathepsin L (Figure 6D; 6F).

C21 Stabilizes Actin Cytoskeleton Integrity and Inhibits Apoptosis in ADR-injured Podocytes *in vitro*

To study the mechanism by which C21 protects ADR-injured podocytes, we examined protein expression before and after treatment of cultured mPODs with ADR in the presence or absence of C21 (1.0 μM) for 24 hours. IF staining for Synpo and Filamentous actin (F-actin) showed that C21 itself did not change expression of these markers in control cells. In contrast, ADR induced prominent podocyte injury, as evidenced by reduced Synpo and diminished F-actin in the cytoplasm, which C21 restored (Figure 7A, Supplementary Figure S3). Silencing of Agtr2 decreased Synpo and F-actin expression, and both Synpo and Agtr2 were further reduced by ADR (Figure 7B, Supplementary Figure S2, S3).

It has been well established that ADR induces podocyte apoptosis *in vivo* and *in vitro* [41, 42]. Here, we verified the apoptotic processes by the protein expression of cleaved Caspase-3 [43]. ADR increased cleaved Caspase-3, which was attenuated by C21, dose-dependently (Figure 7C, western blot). Moreover, ADR-induced cleaved Caspase 3 was further increased in Agtr2 siRNA (Figure 7D).

Next, we examined the expression of cathepsin L in these cells with and without the cathepsin L inhibitor, CAA0225. Silencing of Agtr2 and ADR increased nuclear staining of cathepsin L. C21 treatment reduced the cathepsin L expression stimulated by ADR, and mimicked the effect of CAA0225 (Figure 8A, Supplementary Figure S4).

DISCUSSION

In the present study, we found novel evidence that AT_2R may prevent or ameliorate the development of FSGS and its progression. The major findings from our study are that AT_2R deletion exacerbated experimental FSGS, and the administration of the AT_2R agonist, C21, markedly preserved glomerular morphology, maintained podocyte integrity and reduced albuminuria via the inhibition of glomerular cathepsin L expression. The process by which this may occur is depicted schematically in Figure 8B.

FSGS is characterized by podocyte injury, followed by glomerular sclerosis, and clinically by marked proteinuria and deterioration of kidney function [1]. In our ADR-induced FSGS model [26], we observed that both WT- and AT_2RKO-FSGS mice developed significant hypertension, proteinuria, and glomerular injury compared to their respective controls. ADR induced weight loss in WT mice as reported by others [44], and there was no difference between the WT-FSGS and the AT_2RKO-FSGS mice. Though adult AT_2RKO-Con mice had slightly increased SBP at baseline, as reported previously [9, 29, 31], we did not observe more severe hypertension in AT_2RKO-FSGS as compared with WT-FSGS mice. Following our previous study of AT_2R deficiency, which caused impaired glomerulogenesis and podocyte dysfunction/loss [9, 10], here we confirmed that adult AT_2RKO-FSGS mice developed profound albuminuria, glomerulosclerosis and podocyte injury compared to WT-FSGS mice, suggesting a major role of AT_2R in the development of FSGS and its progression.

In our previous studies [10, 34], we found no apparent differences in levels of Ang II and AT_1R expression (mRNA and protein) in the kidneys of WT as compared with AT_2RKO mice. In the current study, urinary Ang II/Creatine level remained similar between WT and AT_2RKO mice as well. We found no evidence that AT_2R deficiency results in a compensatory change in AT_1R expression. However, further studies are needed to test potential additive effects of C21 and AT_1R blockers on the amelioration of FSGS.

Glomerular cathepsin L is involved in the breakdown of CD2-associated protein (CD2AP), synaptopodin, and dynamin; it contributes to the degradation of glomerular basement membranes and actin cytoskeleton dynamics in podocytes [27, 28]. Of note, cathepsin L-deficient diabetic mice have reductions in albuminuria, mesangial matrix expansion, and tubulointerstitial fibrosis with preserved renal function [45]. Cathepsin L expression is increased in many human glomerular diseases, including diabetic glomerulosclerosis, membranous glomerulonephritis, and FSGS; and it has been suggested that cathepsin L could potentially become a therapeutic target for proteinuric glomerular diseases [45, 46]. Our present report addresses the effect of AT_2R activation on cathepsin L in podocytes. In line with the findings in rats with puromycin aminonucleoside nephrosis [27], our *in vivo* study confirmed increased presence of cathepsin L shown by increased cathepsin L in podocytes of FSGS mice, particularly in AT_2RKO-FSGS mice. These findings lead us to speculate that the activation of glomerular cathepsin L expression might be mechanistically involved in the profound podocyte injury that developed in AT_2RKO-FSGS mice. The mechanism whereby AT_2R activation results in stabilization of cathepsin L expression and/or activity is not clear. Previous studies have shown that inflammatory cytokines up-regulate cathepsin L [40]. Based on our findings of increased glomerular expressions of inflammatory cytokines in AT_2RKO-FSGS mice and their reduction by treatment with the selective, nonpeptide AT_2R agonist C21, it is possible that C21 prevented ADR from stimulating cathepsin L via anti-inflammatory effect of AT_2R.

Our data showed that C21 administration to WT-FSGS mice attenuated systemic hypertension, regardless of when the C21 was administered (Pre. vs. Post) and/or dose (LD vs. HD). Since C21 does not cross the blood–brain barrier [47], it is unlikely that the SBP lowering action of C21 is mediated via AT_2R activation in the central nervous system.

Our findings not only confirmed the general anti-hypertensive effect of C21 summarized by Fatima N et al. [21], but also observed a dose-dependent effect with Pre-C21 and Post-C21 administration.

C21 treatment improved all parameters studied that are related to podocyte injury, independent of urinary Ang II levels. These observations suggest that C21 directly acts on podocytes without altering intrarenal RAS activation. The Pre-C21-HD group showed the most significant improvement among the 4 treatment groups. The Pre-C21-HD group showed most significantly reduced glomerular injury by PAS, as well as improved glomerular mRNA expression of apoptotic and profibrotic genes. In the Pre-C21-HD group, podocyte loss was prevented. These were consistent with the changes of albuminuria, which was reduced most in the Pre-C21-HD group. Considering that morphological changes (heterogeneity) precede the physiological changes, if the treatment duration were longer, Post-C21 might also be as effective as Pre-C21 albuminuria, and it is worth investigating in the future. We unexpectedly found that some parameters, such as SBP, mRNA levels of apoptotic/profibrotic gene expressions in isolated glomeruli, and p57 positive-podocyte numbers were not significantly changed between WT-FSGS and AT_2RKO-FSGS mice, though C21 treatment significantly improved them. We surmise that the limited amount of endogenous production of AT_2R may contribute only partially to ameliorate FSGS mainly via anti-fibrotic effects, but exogenous high-dose C21 administration may exhibit a more potent podocyte protective effect also by anti-apoptotic and cytoskeleton maintenance action.

Our *in vivo* study has certain concerns. First, we studied solely male mice. We acknowledge that the regulation of the RAS exhibits sexual dimorphism, and the *Agtr2* gene is located on the X chromosome [48]. Potential sex-specific influence of AT_2R on FSGS merits further investigation. Next, our AT_2RKO is not podocyte-specific; thus, C21 could affect a number of different cell types within the kidney and elsewhere. There are reports that C21 exhibits direct anti-inflammatory actions in HK2 cells, a human proximal tubular cell line, as well as an anti-fibrotic action on cultured mesangial cells [23, 49]. Thus, we cannot rule out the effect of C21 on other kidney cells, which might have contributed to the improvement of renal morphology and albuminuria. Moreover, although C21 is generally considered as a selective AT_2R agonist, off-target effects have been reported [50]. Also, the dose-dependent decrease of SBP in C21-treated WT-FSGS mice complicates and limits the cause-and-effect interpretation of improved renal morphology and albuminuria with C21, since attenuated systemic hypertension could also reduce the glomerular capillary pressure. Given these concerns, we further sought to explore the impact of ADR and C21 on mPODs *in vitro*.

Our *in vitro* study demonstrated a direct protective effect of C21 on ADR-induced podocyte injury. C21 inhibits ADR's stimulation of cathepsin L which is known to cause the dysregulation of the actin cytoskeleton in podocytes [27]. C21 appeared to work directly on podocytes and preserved podocyte cytoskeletal structure and decreased ADR-induced apoptotic cells in mPODs. Therefore, it may be concluded that C21 ameliorated FSGS at least partly via the direct inhibition of cathepsin L and cell death in podocytes.

In conclusion, the present studies showed that an AT_2R agonist provided renoprotection in experimentally-induced FSGS at least in part through the inhibition of glomerular cathepsin L expression, leading to the maintenance of podocyte integrity, and the prevention of podocyte apoptosis. AT_2R stimulation could potentially become a novel pharmacological tool by which to slow the progression of the nephropathy in FSGS patients.

Supplementary Material

Refer to Web version on PubMed Central for supplementary material.

Acknowledgements

Part of the data was presented as a poster at Kidney Week 2018, the Annual Meeting of the American Society of Nephrology (October 23 to 28, 2018; San Diego, CA, USA).

Funding

This work was supported, in part, by grants from the American Society of Nephrology, Ben J. Lipps Fellowship [2019-2020 (to K.N.M.]; NCATS UCLA CTSI KL2 grant [KL2TR001882 (to Y.M.)] and Cedars-Sinai CTSI Clinical Scholar Grant (to Y.M.); the Canadian Institutes of Health Research [SVB 158606; PJT173534 (to S.L.Z.)]; the Natural Sciences and Engineering Research Council of Canada [RGPIN-2017-05615 (to S.L.Z.)]; and Kidney Foundation of Canada [KFOC190004 (to S.L.Z.)].

Data Availability

The data used to support the findings of this study are available from the corresponding author upon request.

REFERENCE

1. D'Agati VD, Kaskel FJ, Falk RJ. Focal segmental glomerulosclerosis. N Engl J Med. 2011;365(25):2398–411. [PubMed: 22187987]
2. Kitiyakara C, Eggers P, Kopp JB. Twenty-one-year trend in ESRD due to focal segmental glomerulosclerosis in the United States. Am J Kidney Dis. 2004;44(5):815–25. [PubMed: 15492947]
3. Rosenberg AZ, Kopp JB. Focal Segmental Glomerulosclerosis. Clin J Am Soc Nephrol. 2017;12(3):502–17. [PubMed: 28242845]
4. McGrogan A, Franssen CF, de Vries CS. The incidence of primary glomerulonephritis worldwide: a systematic review of the literature. Nephrol Dial Transplant. 2011;26(2):414–30. [PubMed: 21068142]
5. Shankland SJ. The podocyte's response to injury: role in proteinuria and glomerulosclerosis. Kidney Int. 2006;69(12):2131–47. [PubMed: 16688120]
6. Sethna CB, Gipson DS. Treatment of FSGS in Children. Adv Chronic Kidney Dis. 2014;21(2):194–9. [PubMed: 24602468]
7. Kemp BA, Howell NL, Keller SR, Gildea JJ, Padia SH, Carey RM. AT2 Receptor Activation Prevents Sodium Retention and Reduces Blood Pressure in Angiotensin II-Dependent Hypertension. Circ Res. 2016;119(4):532–43. [PubMed: 27323774]
8. Rehman A, Leibowitz A, Yamamoto N, Rautureau Y, Paradis P, Schiffrin EL. Angiotensin type 2 receptor agonist compound 21 reduces vascular injury and myocardial fibrosis in stroke-prone spontaneously hypertensive rats. Hypertension. 2012;59(2):291–9. [PubMed: 22184324]
9. Liao MC, Pang YC, Chang SY, Zhao XP, Chenier I, Ingelfinger JR, et al. AT(2)R deficiency in mice accelerates podocyte dysfunction in diabetic progeny in a sex-dependent manner. Diabetologia. 2021;64(9):2108–21. [PubMed: 34047808]

10. Liao MC, Zhao XP, Chang SY, Lo CS, Chenier I, Takano T, et al. AT2 R deficiency mediated podocyte loss via activation of ectopic hedgehog interacting protein (Hhip) gene expression. J Pathol. 2017;243(3):279–93. [PubMed: 28722118]
11. Liebau MC, Lang D, Bohm J, Endlich N, Bek MJ, Witherden I, et al. Functional expression of the renin-angiotensin system in human podocytes. Am J Physiol Renal Physiol. 2006;290(3):F710–9. [PubMed: 16189286]
12. Suzuki K, Han GD, Miyauchi N, Hashimoto T, Nakatsue T, Fujioka Y, et al. Angiotensin II type 1 and type 2 receptors play opposite roles in regulating the barrier function of kidney glomerular capillary wall. Am J Pathol. 2007;170(6):1841–53. [PubMed: 17525253]
13. Copelovitch L, Guttenberg M, Pollak MR, Kaplan BS. Renin-angiotensin axis blockade reduces proteinuria in presymptomatic patients with familial FSGS. Pediatr Nephrol. 2007;22(10):1779–84. [PubMed: 17530296]
14. Usta M, Ersoy A, Dilek K, Ozdemir B, Yavuz M, Gullulu M, et al. Efficacy of losartan in patients with primary focal segmental glomerulosclerosis resistant to immunosuppressive treatment. J Intern Med. 2003;253(3):329–34. [PubMed: 12603500]
15. Hayashi K, Sasamura H, Nakamura M, Sakamaki Y, Azegami T, Oguchi H, et al. Renin-angiotensin blockade resets podocyte epigenome through Kruppel-like Factor 4 and attenuates proteinuria. Kidney Int. 2015;88(4):745–53. [PubMed: 26108068]
16. Ding G, Reddy K, Kapasi AA, Franki N, Gibbons N, Kasinath BS, et al. Angiotensin II induces apoptosis in rat glomerular epithelial cells. Am J Physiol Renal Physiol. 2002;283(1):F173–80. [PubMed: 12060599]
17. Durvasula RV, Petermann AT, Hiromura K, Blonski M, Pippin J, Mundel P, et al. Activation of a local tissue angiotensin system in podocytes by mechanical strain. Kidney Int. 2004;65(1):30–9. [PubMed: 14675034]
18. Chen S, Lee JS, Iglesias-de la Cruz MC, Wang A, Izquierdo-Lahuerta A, Gandhi NK, et al. Angiotensin II stimulates alpha3(IV) collagen production in mouse podocytes via TGF-beta and VEGF signalling: implications for diabetic glomerulopathy. Nephrol Dial Transplant. 2005;20(7):1320–8. [PubMed: 15840669]
19. Kaschina E, Grzesiak A, Li J, Foryst-Ludwig A, Timm M, Rompe F, et al. Angiotensin II type 2 receptor stimulation: a novel option of therapeutic interference with the renin-angiotensin system in myocardial infarction? Circulation. 2008;118(24):2523–32. [PubMed: 19029468]
20. Matavelli LC, Huang J, Siragy HM. Angiotensin AT(2) receptor stimulation inhibits early renal inflammation in renovascular hypertension. Hypertension. 2011;57(2):308–13. [PubMed: 21189405]
21. Fatima N, Patel SN, Hussain T. Angiotensin II Type 2 Receptor: A Target for Protection Against Hypertension, Metabolic Dysfunction, and Organ Remodeling. Hypertension. 2021;77(6):1845–56. [PubMed: 33840201]
22. Hakam AC, Hussain T. Renal angiotensin II type-2 receptors are upregulated and mediate the candesartan-induced natriuresis/diuresis in obese Zucker rats. Hypertension. 2005;45(2):270–5. [PubMed: 15596573]
23. Dhande I, Ali Q, Hussain T. Proximal tubule angiotensin AT2 receptors mediate an anti-inflammatory response via interleukin-10: role in renoprotection in obese rats. Hypertension. 2013;61(6):1218–26. [PubMed: 23547236]
24. Ruiz-Ortega M, Esteban V, Suzuki Y, Ruperez M, Mezzano S, Ardiles L, et al. Renal expression of angiotensin type 2 (AT2) receptors during kidney damage. Kidney Int Suppl. 2003(86):S21–6. [PubMed: 12969123]
25. Patel SN, Ali Q, Hussain T. Angiotensin II Type 2-Receptor Agonist C21 Reduces Proteinuria and Oxidative Stress in Kidney of High-Salt-Fed Obese Zucker Rats. Hypertension. 2016;67(5):906–15. [PubMed: 27021008]
26. Lee VW, Harris DC. Adriamycin nephropathy: a model of focal segmental glomerulosclerosis. Nephrology (Carlton). 2011;16(1):30–8. [PubMed: 21175974]
27. Kubo A, Shirato I, Hidaka T, Takagi M, Sasaki Y, Asanuma K, et al. Expression of Cathepsin L and Its Intrinsic Inhibitors in Glomeruli of Rats With Puromycin Aminonucleoside Nephrosis. J Histochem Cytochem. 2018;66(12):863–77. [PubMed: 30052474]

28. Keisuke S, Kohei M, Takuji E, Tomoki M, Yuichi M, Rina O, et al. Role of cathepsin L in idiopathic nephrotic syndrome in children. Med Hypotheses. 2020;141:109718. [PubMed: 32289645]
29. Ichiki T, Labosky PA, Shiota C, Okuyama S, Imagawa Y, Fogo A, et al. Effects on blood pressure and exploratory behaviour of mice lacking angiotensin II type-2 receptor. Nature. 1995;377(6551):748–50. [PubMed: 7477267]
30. Nishimura H, Yerkes E, Hohenfellner K, Miyazaki Y, Ma J, Hunley TE, et al. Role of the angiotensin type 2 receptor gene in congenital anomalies of the kidney and urinary tract, CAKUT, of mice and men. Mol Cell. 1999;3(1):1–10. [PubMed: 10024874]
31. Chang SY, Chen YW, Chenier I, Tran Sle M, Zhang SL. Angiotensin II type II receptor deficiency accelerates the development of nephropathy in type I diabetes via oxidative stress and ACE2. Exp Diabetes Res. 2011;2011:521076. [PubMed: 22110472]
32. Sakemi T, Ohtsuka N, Tomiyoshi Y, Morito F. Sex difference in progression of adriamycin-induced nephropathy in rats. Am J Nephrol. 1996;16(6):540–7. [PubMed: 8955769]
33. Grant MKO, Seelig DM, Sharkey LC, Choi WSV, Abdelgawad IY, Zordoky BN. Sexual dimorphism of acute doxorubicin-induced nephrotoxicity in C57Bl/6 mice. PLoS One. 2019;14(2):e0212486. [PubMed: 30785938]
34. Liao MC, Pang YC, Chang SY, Zhao XP, Chenier I, Ingelfinger JR, et al. AT2R deficiency in mice accelerates podocyte dysfunction in diabetic progeny in a sex-dependent manner. Diabetologia. 2021;64(9):2108–21. [PubMed: 34047808]
35. Miyata KN, Lo CS, Zhao S, Liao MC, Pang Y, Chang SY, et al. Angiotensin II up-regulates sodium-glucose co-transporter 2 expression and SGLT2 inhibitor attenuates Ang II-induced hypertensive renal injury in mice. Clin Sci (Lond). 2021;135(7):943–61. [PubMed: 33822013]
36. Miyata KN, Lo CS, Zhao S, Zhao XP, Chenier I, Yamashita M, et al. Deletion of heterogeneous nuclear ribonucleoprotein F in renal tubules downregulates SGLT2 expression and attenuates hyperfiltration and kidney injury in a mouse model of diabetes. Diabetologia. 2021.
37. Mundel P, Reiser J, Zuniga Mejia BA, Pavenstadt H, Davidson GR, Kriz W, et al. Rearrangements of the cytoskeleton and cell contacts induce process formation during differentiation of conditionally immortalized mouse podocyte cell lines. Exp Cell Res. 1997;236(1):248–58. [PubMed: 9344605]
38. Ali R, Patel S, Hussain T. Angiotensin type 2 receptor activation limits kidney injury during the early phase and induces Treg cells during the late phase of renal ischemia. Am J Physiol Renal Physiol. 2021;320(5):F814–F25. [PubMed: 33719572]
39. Wilkening A, Krappe J, Muhe AM, Lindenmeyer MT, Eltrich N, Luckow B, et al. C-C chemokine receptor type 2 mediates glomerular injury and interstitial fibrosis in focal segmental glomerulosclerosis. Nephrol Dial Transplant. 2020;35(2):227–39. [PubMed: 30597038]
40. Kato T, Mizuno S, Kamimoto M. The decreases of nephrin and nuclear WT1 in podocytes may cause albuminuria during the experimental sepsis in mice. Biomed Res. 2010;31(6):363–9. [PubMed: 21187647]
41. Bao H, Ge Y, Peng A, Gong R. Fine-tuning of NFkappaB by glycogen synthase kinase 3beta directs the fate of glomerular podocytes upon injury. Kidney Int. 2015;87(6):1176–90. [PubMed: 25629551]
42. Marshall CB, Krofft RD, Pippin JW, Shankland SJ. CDK inhibitor p21 is prosurvival in adriamycin-induced podocyte injury, in vitro and in vivo. Am J Physiol Renal Physiol. 2010;298(5):F1140–51. [PubMed: 20130121]
43. Hu S, Han R, Shi J, Zhu X, Qin W, Zeng C, et al. The long noncoding RNA LOC105374325 causes podocyte injury in individuals with focal segmental glomerulosclerosis. J Biol Chem. 2018;293(52):20227–39. [PubMed: 30389788]
44. Pereira RL, Buscariollo BN, Correa-Costa M, Semedo P, Oliveira CD, Reis VO, et al. Bradykinin receptor 1 activation exacerbates experimental focal and segmental glomerulosclerosis. Kidney Int. 2011;79(11):1217–27. [PubMed: 21412216]
45. Garsen M, Rops AL, Dijkman H, Willemsen B, van Kuppevelt TH, Russel FG, et al. Cathepsin L is crucial for the development of early experimental diabetic nephropathy. Kidney Int. 2016;90(5):1012–22. [PubMed: 27575559]

46. Sever S, Altintas MM, Nankoe SR, Moller CC, Ko D, Wei C, et al. Proteolytic processing of dynamin by cytoplasmic cathepsin L is a mechanism for proteinuric kidney disease. J Clin Invest. 2007;117(8):2095–104. [PubMed: 17671649]

47. Shraim N, Mertens B, Clinckers R, Sarre S, Michotte Y, Van Eeckhaut A. Microbore liquid chromatography with UV detection to study the in vivo passage of compound 21, a non-peptidergic AT(2) receptor agonist, to the striatum in rats. Journal of neuroscience methods. 2011;202(2):137–42. [PubMed: 21723321]

48. Okumura M, Iwai M, Ide A, Mogi M, Ito M, Horiuchi M. Sex difference in vascular injury and the vasoprotective effect of valsartan are related to differential AT2 receptor expression. Hypertension. 2005;46(3):577–83. [PubMed: 16103268]

49. Koulis C, Chow BS, McKelvey M, Steckelings UM, Unger T, Thallas-Bonke V, et al. AT2R agonist, compound 21, is reno-protective against type 1 diabetic nephropathy. Hypertension. 2015;65(5):1073–81. [PubMed: 25776077]

50. Verdonk K, Durik M, Abd-Alla N, Batenburg WW, van den Bogaerdt AJ, van Veghel R, et al. Compound 21 induces vasorelaxation via an endothelium- and angiotensin II type 2 receptor-independent mechanism. Hypertension. 2012;60(3):722–9. [PubMed: 22802221]

Clinical Perspective

- Classical FSGS is initiated by podocyte injury. Podocytes express angiotensin II type-2-receptor (AT_2R). However, the effects of AT_2R on podocyte injury in FSGS is not known.
- AT_2R deletion exacerbated podocyte injury in the adriamycin-induced murine model of FSGS. The administration of the AT_2R agonist, C21, in mice with FSGS ameliorated podocyte loss and glomerular fibrosis and reduced albuminuria, dose-dependently, most significantly when C21 was given before the FSGS had become established.
- AT_2R may be important as a future therapeutic target for FSGS.

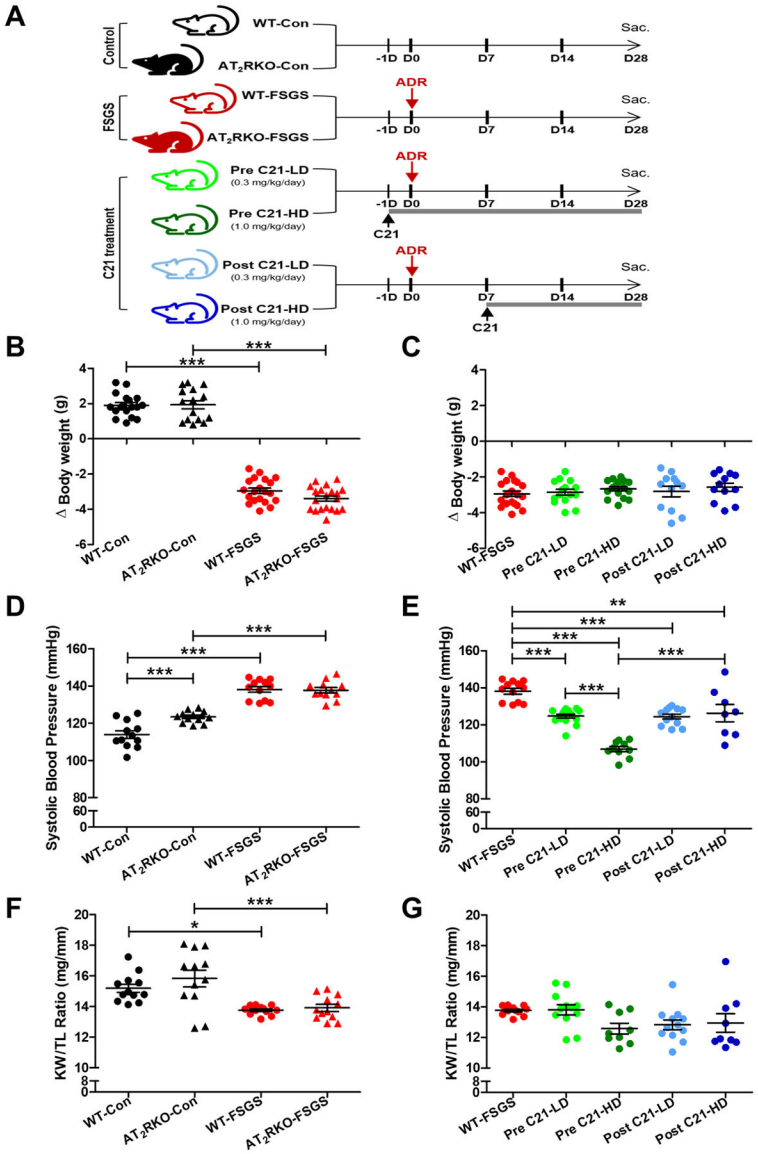

Figure 1. Physiological parameters of FSGS mice with AT_2R deletion and C21 treatment.

(A) Schematic design of the study protocol. Both wild-type (WT) and AT_2RKO mice received adriamycin (ADR) injection to induce FSGS. Separate groups of WT-FSGS mice were treated with either 0.3 (low dose, LD) or 1.0 (high dose, HD) mg/kg/day of Compound 21 (C21), 1-day before (Pre-C21) or 7-day after (Post- C21) the ADR injection. D, day. (B-C) Body weight (g) change at day 28 (N=12–20 in each group). (D-E) Systolic blood pressure (mmHg) at day 28 (N=8–12 in each group). (F-G) Kidney weight (KW)/tibia length (TL) ratio in WT and AT_2RKO mice with and without FSGS (F) and WT-FSGS mice treated with C21 (G) (N=9–12 in each group). Data are mean ± SEM. * p<0.05, ** p<0.01, *** p<0.001.

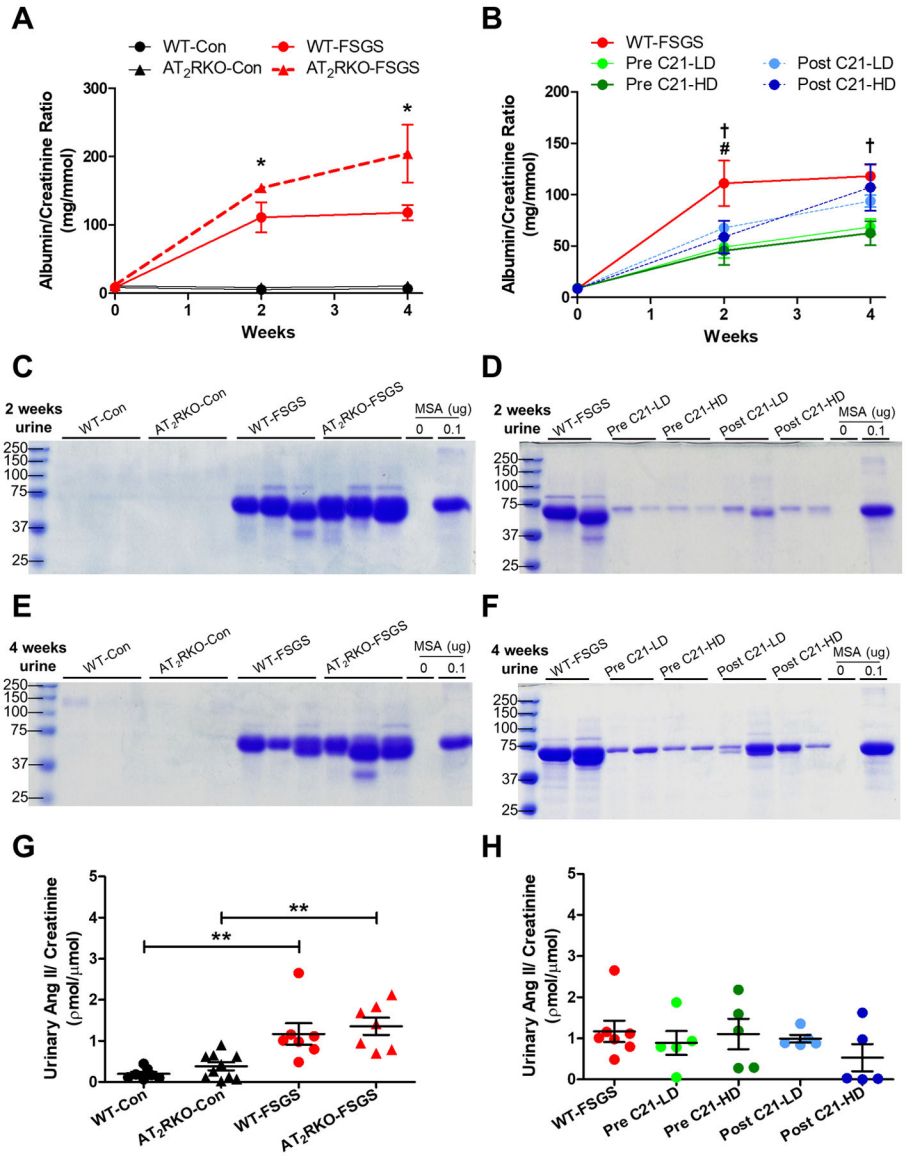

Figure 2. Deletion of AT_2RKO exacerbated and C21 ameliorated ADR-induced FSGS.

(A; C; E; G) WT and AT_2RKO with and without FSGS; (b; d; f; h) WT-FSGS mice treated with C21; (A-B) Longitudinal measurements of urinary ACR (N= 8–13 in each group). * p<0.05 in WT-FSGS vs AT_2RKO-FSGS. # p<0.05 in WT-FSGS vs Pre C21-LD, † p<0.05 in WT-FSGS vs Pre C21-HD; (C-F) Coomassie Blue gel staining of urine at week 2 (C, D) and week 4 (E, F) of FSGS. MSA, mouse serum albumin (μg); (G, H) Urinary Ang II/creatinine value at week 4 of FSGS. Data are mean ± SEM. * p<0.05, ** p<0.01. *** p<0.001.

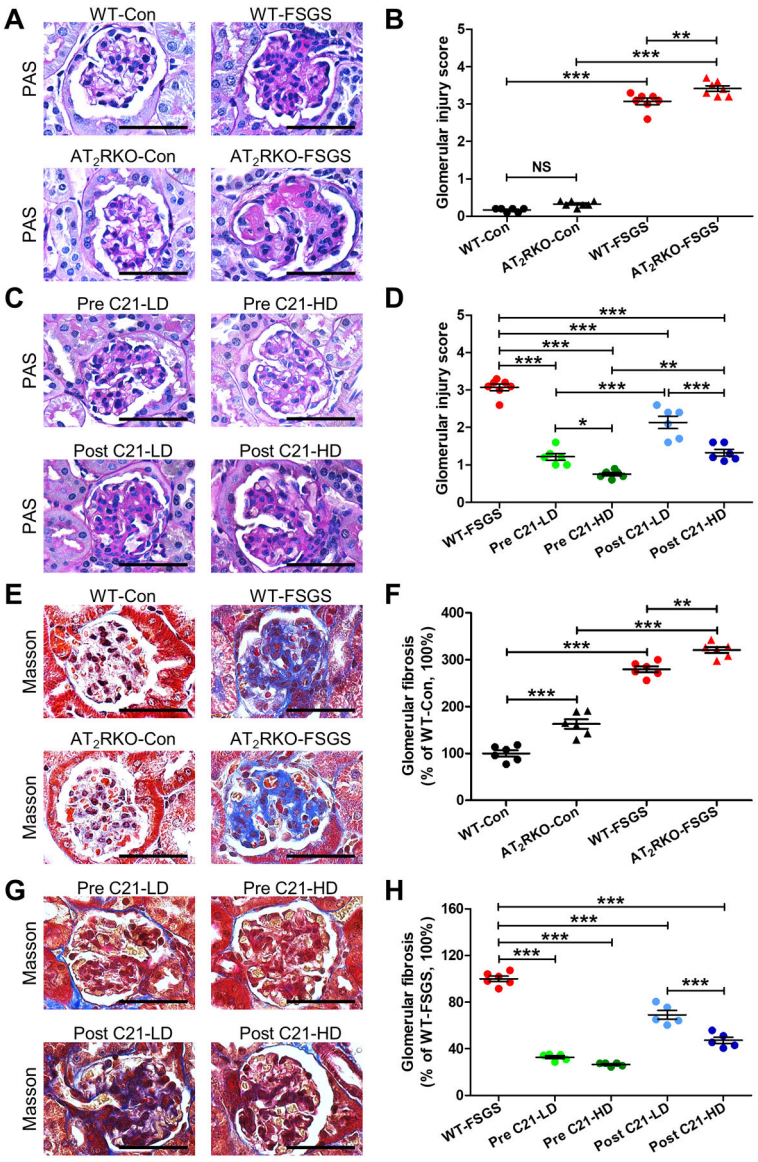

Figure 3. The effect of AT_2R deletion and C21 treatment on renal histology in ADR-induced FSGS.

(A-D) PAS staining of glomeruli in outer cortex in WT and AT_2RKO mice with and without FSGS (A-B) and WT-FSGS mice treated with C21 (C-D). Glomerular injury score based on the PAS images in WT and AT_2RKO mice with and without FSGS (B) and WT-FSGS mice treated with C21 (D). Each mouse is represented by a dot, which is the average of scores of the 30–35 glomeruli (n = 6–7 in each group). (E-H) Masson's trichrome staining of glomeruli in outer cortex in WT and AT_2RKO mice with and without FSGS (E-F) and WT-FSGS mice treated with C21 (G-H) and the quantification of glomerular fibrosis (F, H). Scale bar, 50 μm; Data are mean ± SEM. * $p<0.05$, ** $p<0.01$, *** $p<0.001$.

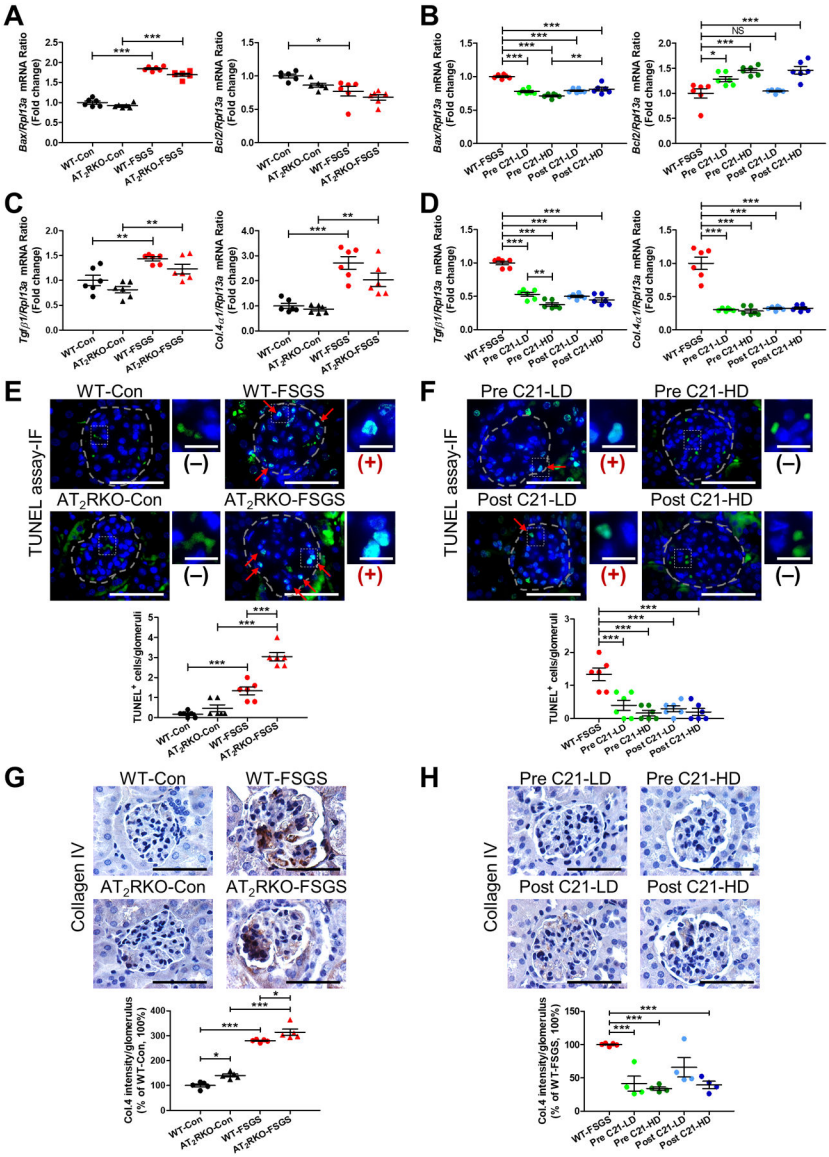

Figure 4. The effect of AT_2R deletion and C21 treatment on glomerular molecular changes in ADR-induced FSGS.

(A-D) RT-qPCR of *Bax* and *Bcl2* mRNA (A, B) and *Tgf-β1* and *Col4α*1 mRNA (C, D) in freshly isolated glomeruli. *Rpl13α* was used as a reference gene. Data are mean ± SEM, N=6 mice per group. (E; F) TUNEL staining of glomeruli in WT and AT_2RKO mice with and without FSGS (E) and WT-FSGS mice treated with C21 (F) and their semi-quantifications. Scale bar, 50 μm; (−) TUNEL negative staining; (+) TUNEL positive staining. Scale bar, 10 μm; (G; H) Collagen IV-IHC staining of glomeruli in WT and AT_2RKO mice with and without FSGS (G) and WT-FSGS mice treated with C21 (H) and their quantifications. Scale bar, 50 μm; Data are mean ± SEM. N=4–5 mice in each group; * $p<0.05$, *** $p<0.001$.

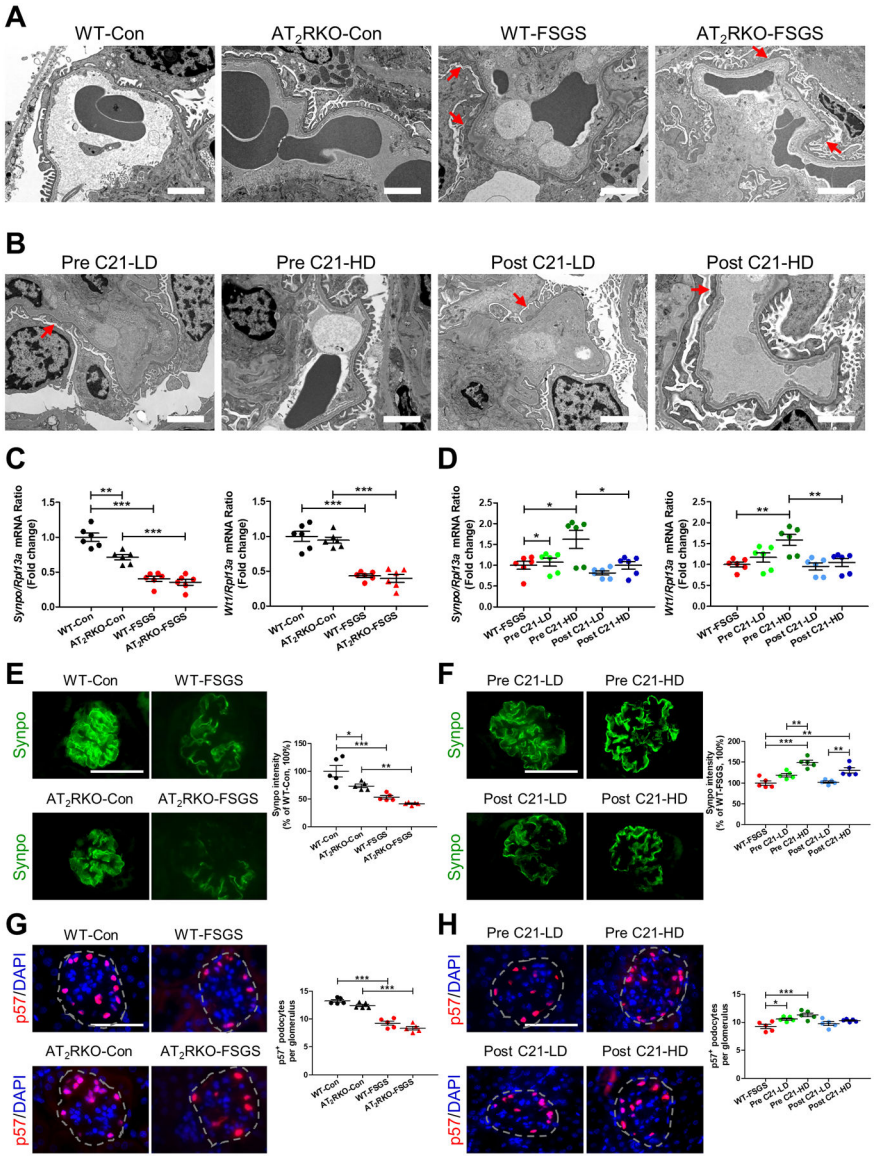

Figure 5. The effect of AT_2R deletion and C21 treatment on podocyte injury in ADR-induced FSGS.

(A; C; E; G) WT and AT_2RKO with and without FSGS; (B; D; F; H) WT-FSGS mice treated with C21; (A-B) Electron microscopy. Original magnification x5000. Scale bar, 2 μm; (C-D) RT-qPCR of synaptopodin (*Synpo*) and Wilms tumor 1 (*Wt-1*) mRNA in freshly isolated glomeruli. *Rpl13α* was used as a reference gene; (E; F) Synpo-IF staining and their quantifications (N=5 in each group). (G-H) Podocyte number per glomerular section based on p57-positive cells (red) in glomeruli of the kidneys with DAPI (blue). Each mouse is represented by a dot, which is the average of the p-57 positive cells in 30–35 glomeruli (N = 4–6 mice in each group). Scale bar, 50 μm; Data are mean ± SEM. * $p<0.05$, ** $p<0.01$, *** $p<0.001$.

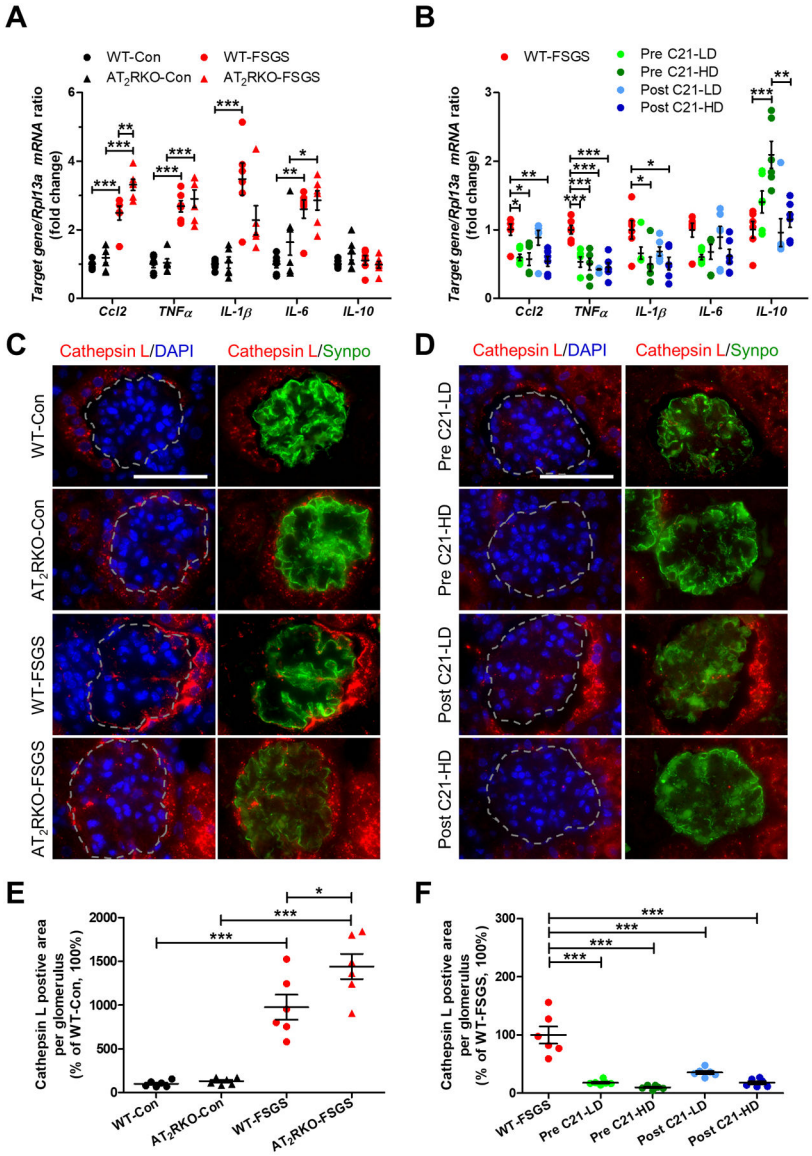

Figure 6. The effect of AT_2R deletion and C21 treatment on glomerular cathepsin L expression in ADR-induced FSGS.

(A; B) RT-qPCR of inflammatory cytokines (C–C motif chemokine ligand 2 (*Ccl2*), tumor necrosis factor-*α* (*TNF-α*), *interleukin (IL)-1β, IL-6, and IL-10)* in freshly isolated glomeruli. *Rpl13a* was used as a reference gene; (C; D) Co-IF staining of glomerular cathepsin L (red) and the merge with Synpo (green) or DAPI (blue) in WT and AT_2RKO mice with and without FSGS (C) and WT-FSGS mice treated with C21 (D). Scale bar, 50 μm. (E; F) Semi-quantification of cathepsin L positive staining area/glomerular area (N=6 in each group). Data are mean ± SEM. * $p<0.05$, *** $p<0.001$.

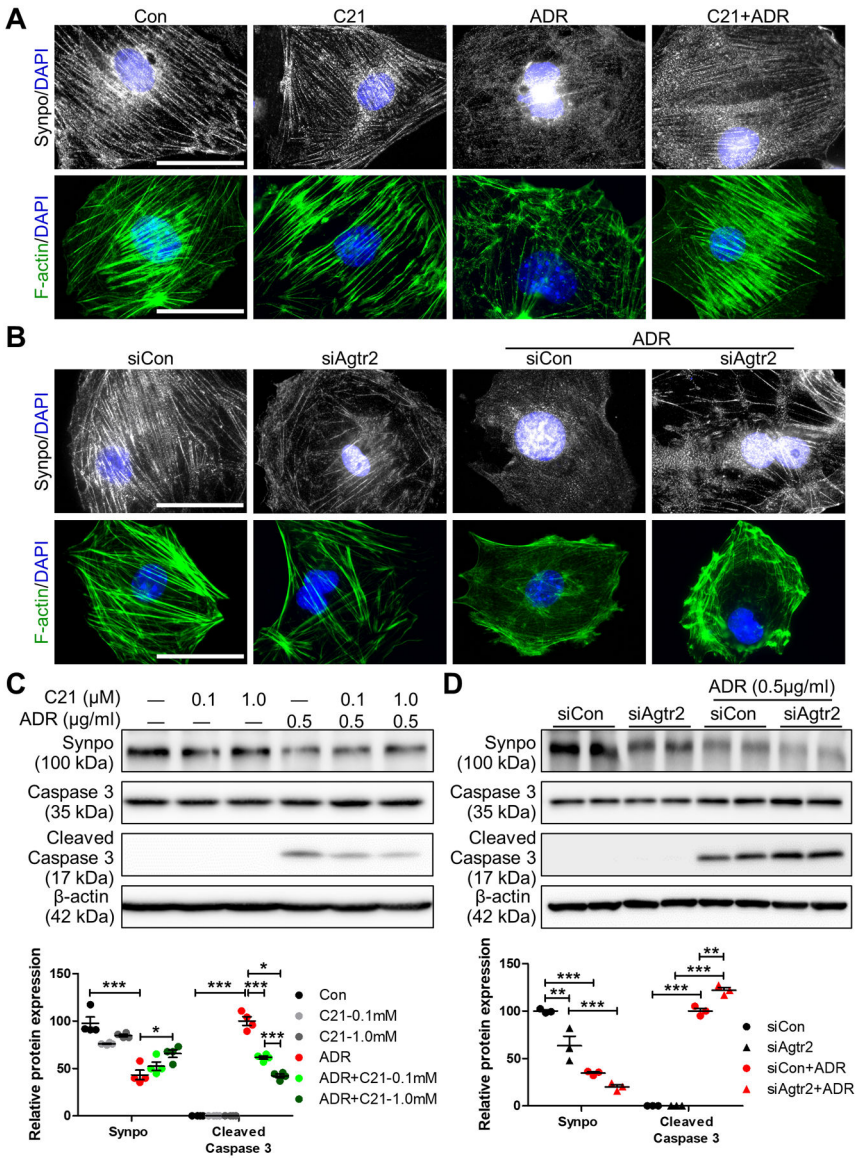

Figure 7. Podocyte integrity and apoptosis induced by ADR *in vitro*.

(A) Synpo-IF (upper panel, white) and F-actin-IF (lower panel, white) with DAPI (blue) in mPODs, in the presence or absence of C21 and/or ADR. (B) Effect of Agtr2 siRNA (siAgtr2) or scrambled siRNA (siCon) with and without ADR on Synpo and F-actin expressions. (C) Western blot analysis in mPODs with and without ADR, treated with different doses of C21 for 24 hours. (D) Western blot analysis in mPODs with siAgtr2 vs siCon with and without ADR. Scale bar, 50 μm. Data are mean ± SEM. * $p<0.05$, *** $p<0.001$.

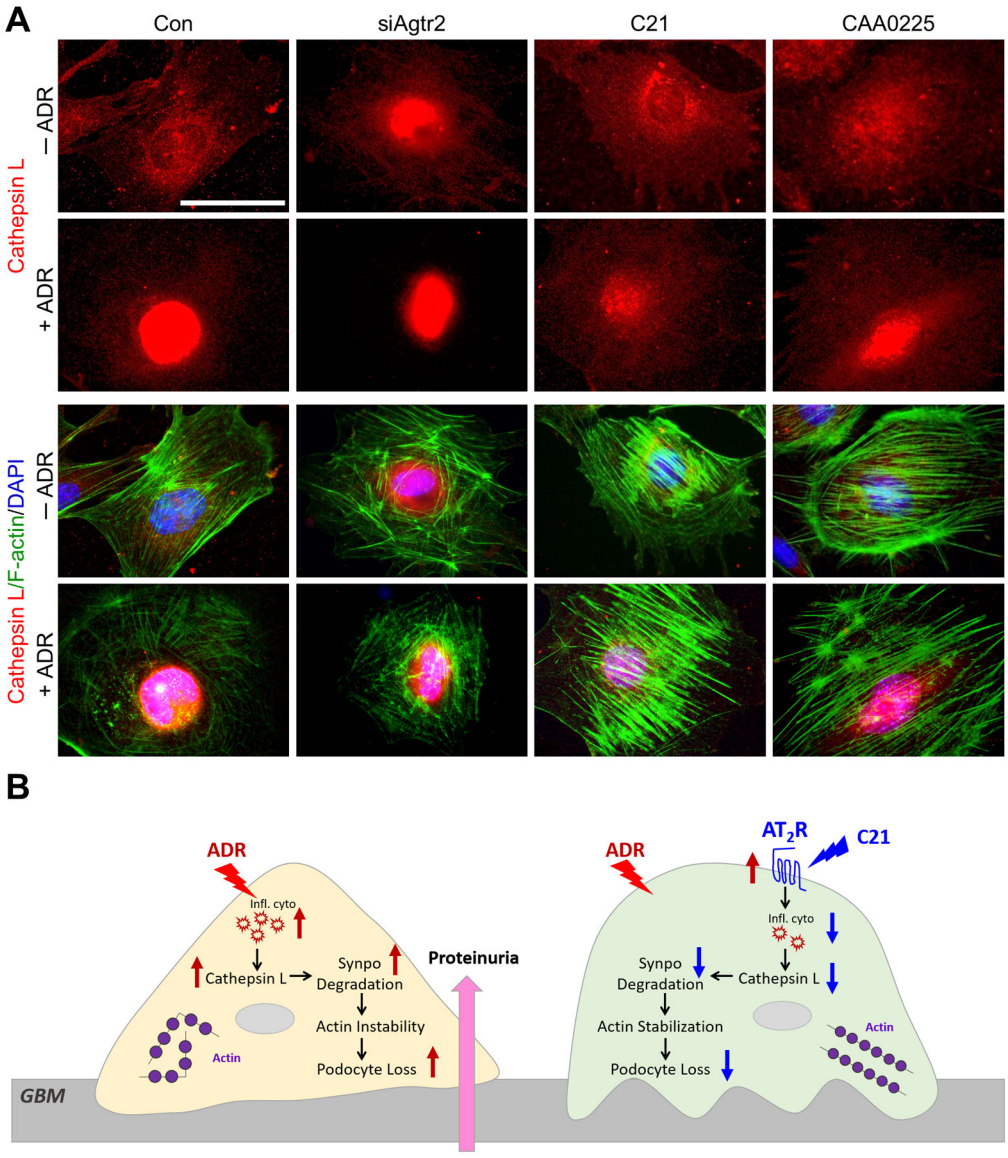

Figure 8. ADR increases and C21 decreases Cathepsin L expression

(A) Co-IF staining of Cathepsin L (red) and the merge with F-actin (green) and DAPI (blue) in mPODs *in vitro*. Control, Agtr2 siRNA (siAgtr2), C21-treated, and CAA0225 (a cathepsin L inhibitor)-treated cells were assessed with and without ADR. Scale bar, 50 μm. (B) A schematic illustration of how Cathepsin L potentially mediates the podocyte actin instability and proteinuria in AT_2R deletion on FSGS development in mice; and how the administration of AT_2R agonist (C21) would ameliorate FSGS-induced podocyte injury. In brief, increased inflammatory cytokines (infl. cyto) by ADR likely stimulate Cathepsin L expression, which causes podocyte actin instability, leading to podocyte loss (left orange podocyte). In contrast, C21 prevents the ADR-induced inflammatory cytokines and Cathepsin L expression, thereby maintaining the podocyte integrity (right green podocyte).